

RESEARCH PAPER

Magnetic Metal Nanoparticles Decorated Ionic Liquid with Excellent Antibacterial Activity

Hadi Salari¹, Moslem Karimi Asl², Mohsen Padervand³, Mohammad Reza Gholami^{2*}

¹ Department of Chemistry, College of Sciences, Shiraz University, Shiraz, Iran

² Department of Chemistry, Sharif University of Technology, Tehran, Iran

³ Department of chemistry, Faculty of Science, University of Maragheh, Maragheh, Iran

ARTICLE INFO

Article History:

Received 06 March 2020

Accepted 28 May 2020

Published 01 July 2020

Keywords:

Antibacterial activity

Escherichia coli

Ionic Liquids

Magnetic nanoparticles

Staphylococcus aureus

ABSTRACT

Fe₃O₄ magnetic structure was synthesized with co-precipitation method. Surface of magnetic core was modified with hydrophobic BMIM[PF₆] ionic liquid. The samples became antibacterial by loading gold, copper and silver nanoparticles and denoted as Fe₃O₄/IL/X (X=Ag, Au, Cu). X-ray diffraction (XRD), scanning electron microscopy (SEM), energy dispersive X-ray (EDX), thermal gravimetric analysis (TGA), Atomic absorption spectroscopy (AAS), Fourier transform infrared (FTIR) and vibration sample magnetometer (VSM) techniques were applied for catalysts characterization, metal concentration analysis and morphology monitoring. Modified nanostructures were used for inactivation of Escherichia coli as the gram negative and Staphylococcus aureus as the gram positive of bacteria. Transmission electron microscopy (TEM) images indicated that highest bacteria cell walls destruction is achieved when the surface of the magnetic nanostructure is coated with gold particles. Hydrogen bonds between cell wall and ionic liquid and gradual release of metals from Fe₃O₄/IL surface facilitate the metals arrive to outer layer of bacteria. Minimum inhibitory concentration (MIC) study approved the positive effect of ionic liquid.

How to cite this article

Salari H., Karimi Asl M., Padervand M., Gholami MR. Magnetic Metal Nanoparticles Decorated Ionic Liquid with Excellent Antibacterial Activity. J Nanostruct, 2020; 10(3): 613-623. DOI: 10.22052/JNS.2020.03.015

INTRODUCTION

Fe₃O₄ based nanomaterials have drawn much attention in many academic and industrial fields like immunoassays, imaging, catalysis, biomedical and biochemical engineering [1-3]. Special focus has been concentrated for utilizing of novel Fe₃O₄ multifunctional compounds due to their fitness and chemical stability. In antibacterial investigation and study, the reused ability of functionalized nanosized Fe₃O₄ is a key factor. Furthermore, modification of magnetic materials surface for increasing their stability is very important. There are several factors such as: oxidation by air and

erosion by acid and base which could alter the structure and contexture of magnetic particles [4-10].

In latter years, metal nanostructures have attracted much attention due to their extremely high surface to volume ratio. They increase the catalytic activity and by using of metal nanoparticles as catalyst, amount of materials will be reduced in catalysis and organic synthesis [11-15]. One of the problems during catalysis is aggregation of nanomaterials. For solving this problem, nanoparticles should be stabilized by immobilization on support [16,17]. An important method which improved recently is using of ionic

* Corresponding Author Email: hsalari@shirazu.ac.ir
gholami@sharif.ir

liquids (ILs) for coating of these particles. Metal nanoparticles can be formed and stabilized by ILs [17]. They possess an intrinsic high charge and polarizability which allow them to produce electrostatic and steric stabilization [17-19].

Nanoscience has expanded its valuable applications in biomedical fields including fighting and preventing diseases using functional atomic scale materials. Different nanoparticles have been considered to sensitize the resistant strains of bacteria to the most potent antibiotics. The bactericidal effects of different nanosized particles depend mainly to the size and shape of the particles. Smaller particles are better in inactivity due to direct interaction with a bacteria.

Room temperature ionic liquids (RTILs), are recognized as a class of new media with attractive applications in separation, synthesis and catalysis. RTILs which are known as designer and green solvents have unique chemical and physical properties like low vapor pressure, non-flammability, stability and solubility in organic and inorganic solvents [20-23]. One of the main challenge in application of ionic liquids is availability and cost issues. Ionic liquids supported catalysts offer an absorbing opportunity to have economic heterogeneous structure and bring many advantages like easier separation and re-utilization [17]. By coating the catalyst surface with small amount of RTILs, catalyst react as a multiphase system which lead to higher selectivity and conversion.

Supported ILs catalysts have been developed. Ionic liquids immobilization can be done by covalent anchoring, physisorption, polymerization and sol-gel [24]. Supported ILs catalysis has been used for a variety of catalysis and electrochemistry areas. Because of low volatility, they are especially useful in gas-phase systems. The recent development in supported ILs materials have demonstrated an immense potential in commercial processes.

In this work we aimed at preparation, characterization and investigation of antibacterial activity of Au, Ag and Cu metal nanoparticles contained hydrophobic ionic liquid (butylmethylimidazolium hexafluorophosphate (BMIM[PF₆])) modified Fe₃O₄. The produced catalysts indicated high antibacterial activity and TEM images proved cell walls destruction. The effect of initial cell concentration, composite dosage was discussed and the interactions of noble metal with the bacteria were studied.

MATERIALS AND METHODS

Chemicals including methanol, FeCl₃·6H₂O, FeCl₂·4H₂O, HCl, NaOH, BMIM[PF₆], AgNO₃, HAuCl₄·6H₂O, Cu(NO₃)₂ and all of other chemicals were purchased from Merck Co. (Germany) and used without any further purification. The working solutions were supplied weekly by making the standard solution with distilled water and more diluted working solutions were prepared daily by diluting this solution with double distilled water. Nitrogen gas (purity of 99.99%) was applied for creating the inert atmosphere which is necessary for synthesis of Fe₃O₄.

Preparation of Fe₃O₄

Magnetic particles were synthesized as described in the literature [25]. Briefly, 2.6 g of FeCl₃·6H₂O and 1 g FeCl₂·4H₂O and 0.4 mL concentrated HCl were dissolved in 20 mL water under N₂ atmosphere. After 1h stirring, this solution was added drop wise into 200 mL of sodium hydroxide solution (0.8 M) under the N₂ gas. The mixture was vigorously stirred for 60 min with 1200 rpm. The prepared black precipitate was separated using a strong magnet. The decanted solid sample was washed with water and ethanol and dried for 6 h at 70 °C.

Preparation of Fe₃O₄/IL

Impregnation method was applied for Fe₃O₄/IL production [26]. 1 gr of solid powder ultrasonicated for 30 min in ethanol, then BMIM[PF₆] (0.5 gr) was added and the suspension stirred for 6 h. After this time, produced material filtrated with filtering paper and the solid washed with absolute ethanol, and dried at 50 °C overnight.

Preparation of Fe₃O₄/IL/X

Total amount of the desired ionic liquid-modified magnetite nanoparticles was dissolved in 100 mL of water and sonicated for 20 min. The solution was mechanically stirred. Then 25 mL of 0.01 M AgNO₃ in water was added. The mixture was stirred for 8 h, and then 25 mL of 0.01M NaBH₄ was added. After stirring for 4 h, the supported Ag nanoparticles were magnetically separated. Final brown Powder which is denoted as Fe₃O₄/IL/Ag washed twice with water and ethanol respectively and dried for 6h at 70 °C. Other materials (Fe₃O₄/IL/Au and Fe₃O₄/IL/Cu) were prepared by similar method with their relative solutions. The yield for samples were 93-98%.

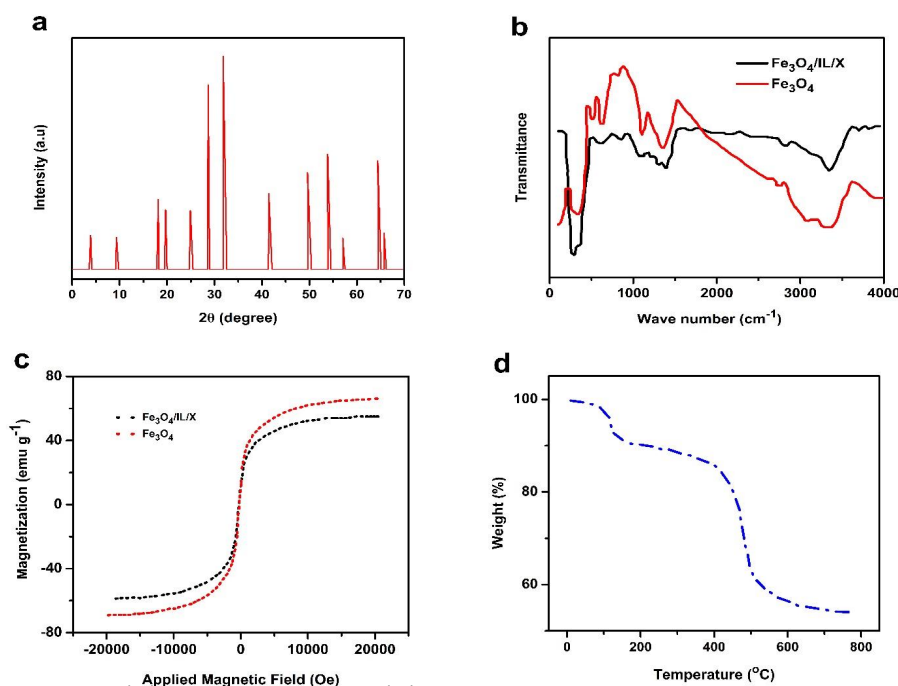


Fig. 1. XRD pattern of $\text{Fe}_3\text{O}_4/\text{IL}/\text{X}$ (a), FTIR spectra of $\text{Fe}_3\text{O}_4/\text{IL}/\text{X}$ and Fe_3O_4 (b), Magnetization curves of prepared samples (c) and TGA curve of $\text{Fe}_3\text{O}_4/\text{IL}/\text{X}$ (d).

Antibacterial test

Specified colony-forming units (CFU mL^{-1}) of bacteria cell concentration have been prepared for antibacterial experiments. A certain amount of bacteria suspension (40 mL) and composites (30 mg), was stirred in Petri dish mechanically [27]. Every 30 minutes, 1 mL of the mixture was diluted with 1% saline. Specific amount of diluted sample was incubated at 37 $^{\circ}\text{C}$ for 24 h on soybean casein digest agar. Then counting of remaining colonies was done.

For investigation of cell wall alteration, TEM analysis was done. 20 mg solid was mixed with 10^7 CFU mL^{-1} cells. After 120 min, the cell suspension collected and centrifuged down to a pellet. 2.5% glutaraldehyde was used for growing bacteria for 12 h. The temperature kept at 4 $^{\circ}\text{C}$. Phosphate buffer and aqueous solution of $\text{Na}_2\text{H}_5[\text{P}(\text{W}_2\text{O}_7)_4]$ were applied for washing and coloring the specimens. The samples were placed onto the copper grids with holey carbon films for TEM test (Philips CM200) [27].

RESULTS AND DISCUSSION

XRD pattern of $\text{Fe}_3\text{O}_4/\text{IL}/\text{X}$ nanostructures, presenting the characteristic peaks of Fe_3O_4 structure with five characteristic peaks, which

reveal iron oxide phase ($2\theta = 32, 42, 51, 54, 64$); these are related to their corresponding indices of (112), (220), (024), (303), (224). It can be seen that the diffraction peaks of $\text{Fe}_3\text{O}_4/\text{IL}/\text{X}$ are similar to those of the parent Fe_3O_4 nanoparticles, which suggests that no excess crystalline phase appears after the surface modification and metal particle loading (Fig. 1a).

Magnetic particles can be verified by wide strong absorption band between 460 and 500 cm^{-1} and for Fe-O bond of bulk magnetite at 570 cm^{-1} . The peaks at 1560, 1400, 1320 and 1250 cm^{-1} could correspond to aromatic C-N stretching and the peaks around 2980 and 2900 cm^{-1} can be assigned to the asymmetric and symmetric vibrations of C-H, respectively. The broad peak between 3000 and 3500 cm^{-1} in Fig. 2b shows the hydrogen bond forming in ionic liquids analogous. The hydrogen bonds formed in system $\text{BMIM}[\text{PF}_6]-\text{Fe}_3\text{O}_4$ is the O...H and F...H. The weak peak between 2875 and 2940 cm^{-1} in the Fig. 2b also shows the hydrogen bonds H-O...H exist. The peak at 1440 cm^{-1} is ascribed to C=N stretching vibration.

Magnetic properties of prepared samples are shown in Fig. 2c. Fe_3O_4 and $\text{Fe}_3\text{O}_4/\text{IL}/\text{X}$ have magnetic saturation values of 67 and 52 emu/g respectively. Modification of Fe_3O_4 surface by

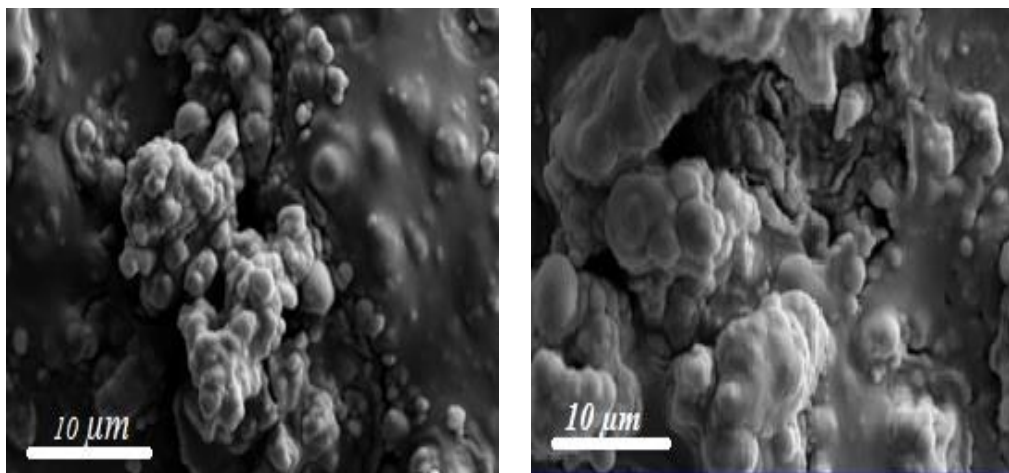


Fig. 2. SEM images of $\text{Fe}_3\text{O}_4/\text{IL}$.

ionic liquid reduces the magnetic saturation a little. Superparamagnetic features for all samples are seen from magnified hysteresis loops. With this high magnetization, $\text{Fe}_3\text{O}_4/\text{IL}/\text{X}$ are well re-dispersed samples with suitable response to external magnetic field. TGA analysis of catalyst which is presented in Fig. 1d demonstrates that 45 weight percent of catalysts are included ionic liquid.

Scanning electron microscopy (SEM) images (Fig. 2) show the morphological character of ionic liquid modified Fe_3O_4 . Fig. 3 demonstrates the SEM images of $\text{Fe}_3\text{O}_4/\text{IL}/\text{X}$ nanostructures. The size of each nanoparticles is in the range of 40-60 nm. These images also demonstrate high dispersion without aggregation and approximately uniform in size distribution. As can be seen the nanoparticles have spherical shapes. EDX analysis showed that weight percent of gold, silver and copper were 3.2, 3.1 and 3.2 respectively.

The results of antibacterial activity over different composites are shown in Fig. 4. Au contained $\text{Fe}_3\text{O}_4/\text{IL}$ has shown the highest inactivation activity, but no activity was observed for Fe_3O_4 and $\text{Fe}_3\text{O}_4/\text{IL}$. The antibacterial activity of $\text{Fe}_3\text{O}_4/\text{IL}/\text{X}$ are related to releasing of Ag, Au and Cu in medium. Fig. 5 shows the TEM images of destroyed cell after 150 min treatment. Adhesion of nanocomposites on to the layer of the membrane is the main reason for inactivation of microorganism. With attaching the nano noble metal to cell wall, some different processes undergo lead microorganism interrupting. The

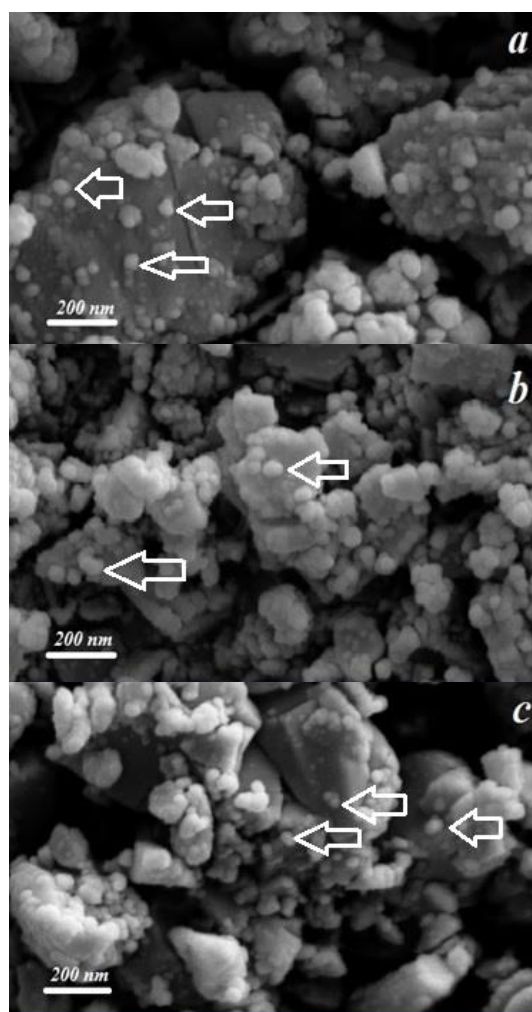


Fig. 3. SEM images of a) $\text{Fe}_3\text{O}_4/\text{IL}/\text{Au}$, b) $\text{Fe}_3\text{O}_4/\text{IL}/\text{Cu}$ and c) $\text{Fe}_3\text{O}_4/\text{IL}/\text{Ag}$.

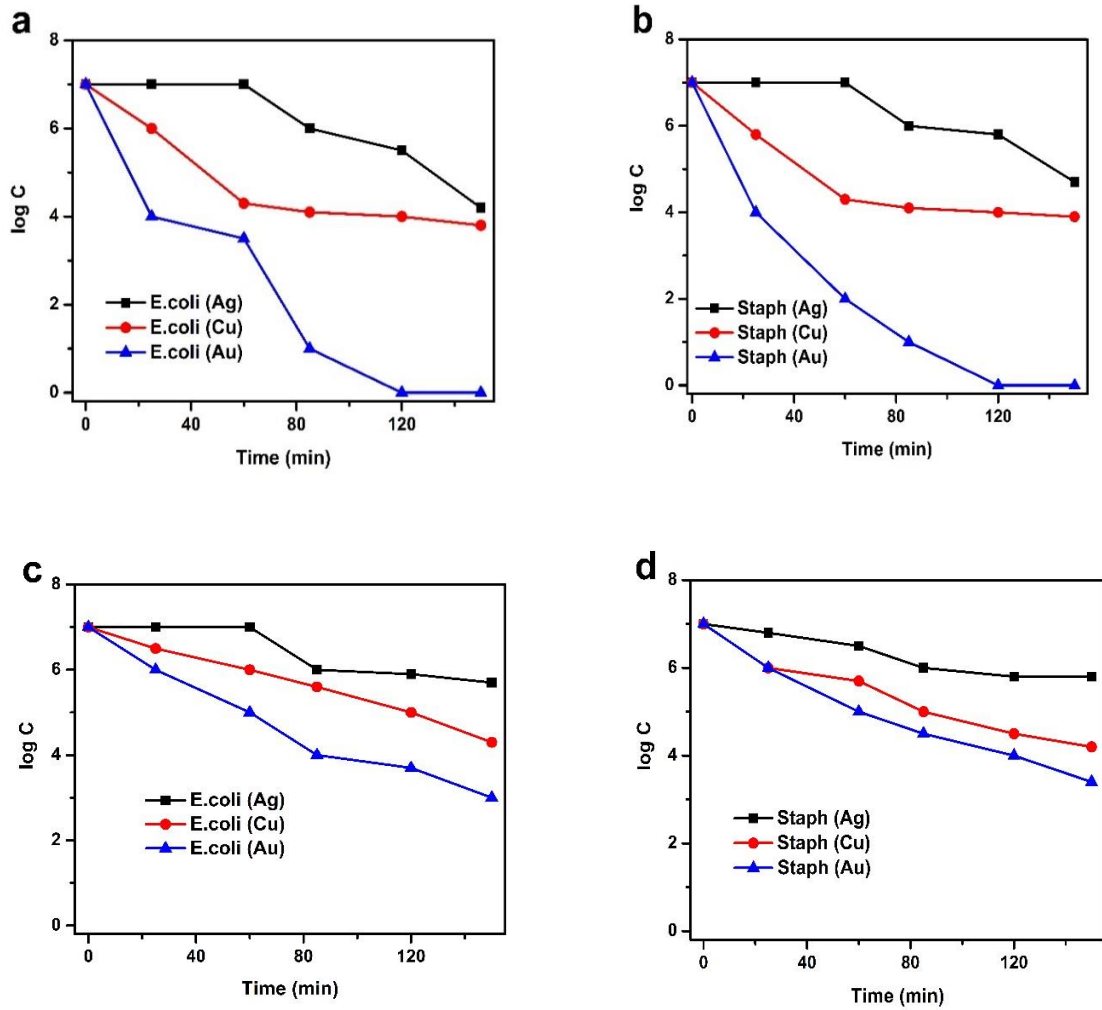


Fig. 4. Antibacterial activity of $\text{Fe}_3\text{O}_4/\text{IL}/\text{X}$ (a,b) and Antibacterial activity of $\text{Fe}_3\text{O}_4/\text{X}$ (c,d) . [catalyst]=250 ppm, [cell]= 10^7 CFU mL^{-1} .

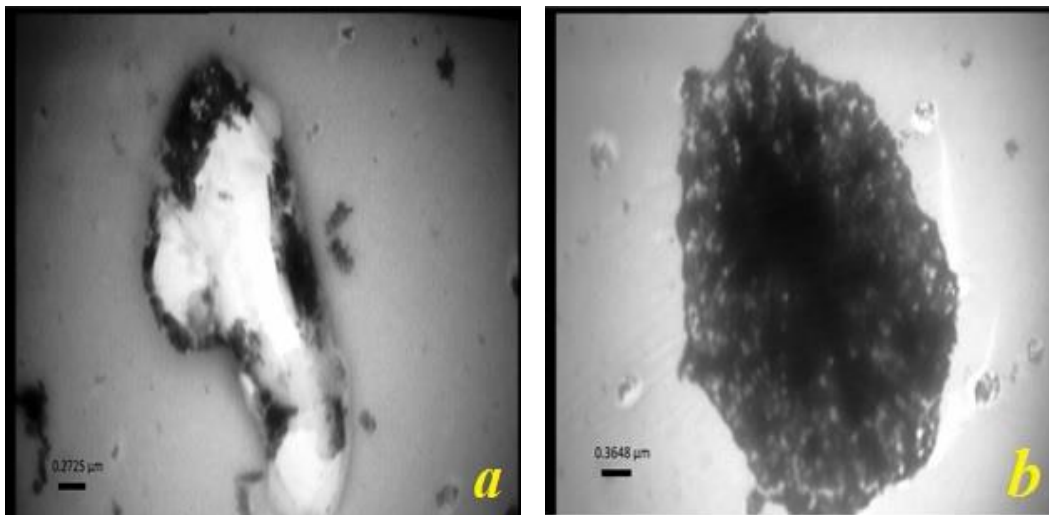


Fig. 5. TEM images of the cell walls after the treatment time ((a) *E. coli* cell and (b) *S. aureus* cell).

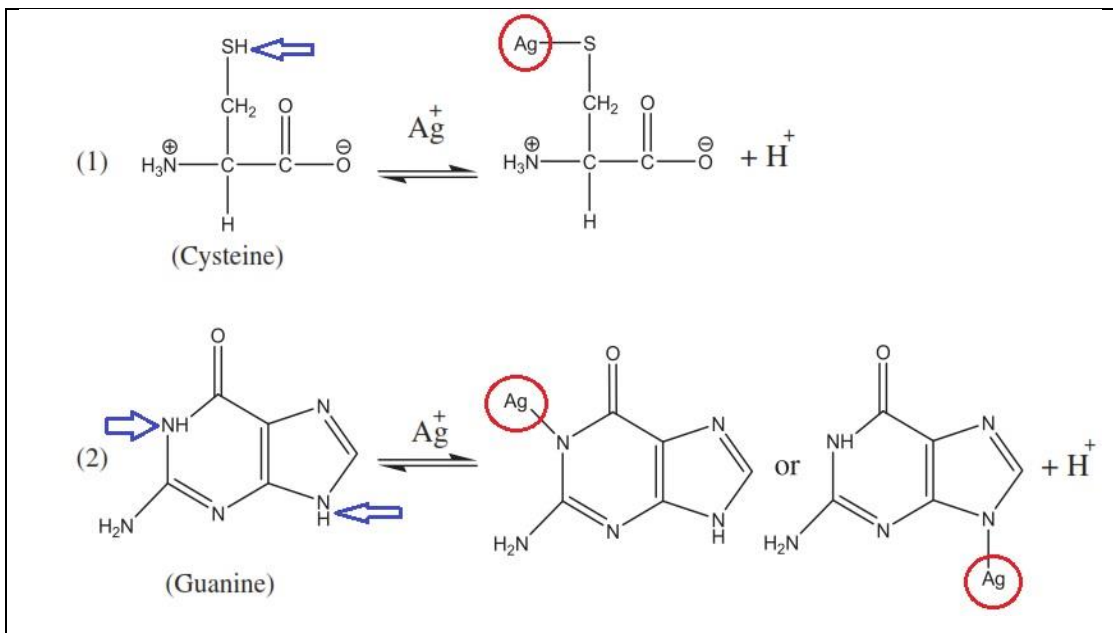


Fig. 6. Silver ion effect on Cysteine (1) and Guanine (2).

overall charge of bacterial cells at biological pH values is negative because of presence of carboxylic groups in the lipoproteins. Escherichia coli (E. coli) and Staphylococcus aureus (Staph) have high anionic charge density that enable them interact easily with metal in environment [28,29]. Because of larger radius of gold ion, they grafted to the ionic liquid weaker than Silver and Copper. Hence, realizing of Au are more than Cu and Ag. It is logical to state that nanoparticles have large surface area available which enhanced the interactions and bactericidal affect than the large size particles.

Colony formation of bacteria will be prevented if the silver ion concentration be higher than 10^{-5} M. The presence of Ag was corroborated by atomic absorption spectroscopy (AAS). Atomic absorption analysis approved the other metals presence in solution. Cross-linking of the DNA helix, binding of Ag^+ ion to nitrogen atom of Guanine in DNA and interaction of silver ion with thiol group of Cysteine are some explanation for inactivation [30-34]. Silver ion with forming a complex with Cysteine by replacing the hydrogen atom of thiol with Ag, disturbed the enzymatic function of protein (Fig. 6).

The outer membrane of gram negative cell wall contains Mg and Ca which contribute to the outer membrane. If these metals replaced by outer vice

versa ions, the loss of lipopolysaccharide may occur. Some enzyme like 5-Nucleotidas released generally by osmotic shock [35]. Metal transferred to cell structure can active these enzymes. Negative gram bacteria cell wall such as E. coli may disturbed with this process. Adhering of Ag, Au and Cu to microorganism cell wall can block the pores which lead to nourish preventing [36]. Presence of fluoride in PF_6^- anion of $\text{BMIM}[\text{PF}_6]$ has major role for adsorbing the bacteria by hydrogen bonding and occurrence of this phenomenon.

E. coli composed of two-layer lipid (lipoproteins, lipopolysaccharids, phospholipids and proteins) with about 7 nm thickness. Lipopolysaccharides are centered in the outer membrane of cell wall and consist of a certain lipid (lipid A). We suggest the hydrogen bonding between PF_6^- anion of ionic liquid and head of lipid form some channels where Au, Ag and Cu can be transferred to the microorganism (Fig. 7). Ag, Au and Cu can penetrate in to cell structure via some transmembrane proteins [37]. Researcher discovered that extracted granules were in part composed of sulfur and silver [38]. Because of leaking the cytoplasm and dehydration and shrinking the bacteria cells, damaging was occurred.

Copper has the capacity to kill bacteria by membrane destroying due to strong reduction ability, which can extract electrons from the

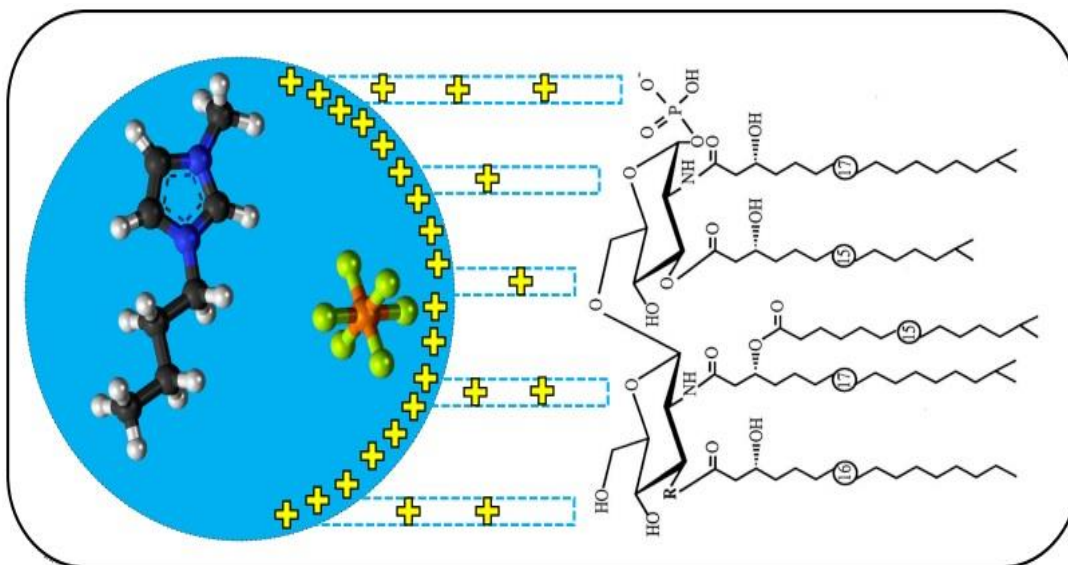


Fig. 7. Movement of metals to cell wall.

bacteria cause escaping and oxidizing of the cell nucleus [39]. When the Cu concentration is high enough, eluted ions from surface nanoparticles are absorbed by bacteria.

Gold nanoparticles exert their antibacterial treatment mostly by i) membrane potential change and inhibit ATP synthase activities to decrease the ATP level lead to decline in metabolism, ii) ribosome subunit inhibition for tRNA binding results in collapse of biological process [40].

Staph is a positive gram bacteria. The cell wall in this kind of bacteria is thick (15-80 nm), consists of several layers of peptidoglycan which make positive gram bacteria protective against exotic agents. We may expect that E. coli as a gram negative bacteria damaged easier than Staph as a gram positive bacteria by their interaction with Au, Cu and Ag nanoparticles. The results reported in Fig. 4 emphasize that $Fe_3O_4/IL/X$ can destroy E. coli and Staph with similar rate. Potential of these samples for positive gram bacteria disruption is very interesting. Peptidoglycan is a negative charge group. Thus Ag, Au and Cu ion could get trapped by the cell wall of Staph. Bmim[PF₆] ionic liquid by strong hydrogen bonding donor group can strongly stick to cell wall. By forming direct channel to microorganism and transferring the metals, these noble metals could penetrate to cell and disturb it.

For reuse testing, after each consideration, the

solid recovered by a strong magnet (1.5 T), washed with water and ethanol two times respectively, dried at 70 °C for 8h and used again. Reused ability of $Fe_3O_4/IL/X$ nanostructures for inactivation of Staphylococcus aureus after three times are presented in Fig. 8. Because of smaller radius of silver ions they grafted to ionic liquid stronger than copper and gold cations, result in slower releasing from surface with steep slope. Similar trends observed for inactivation of Escherichia coli.

The results of Minimum inhibitory concentration (MIC) in terms of different dosage of catalyst from 150 to 750 ppm are presented in Fig. 8. From these data it can be seen that resistance of E.coli and Staph decreased with increasing the nanoparticle concentration. As shown in Fig. 9, the MIC for $Fe_3O_4/IL/Au$ was 150 ppm to E. coli. The MIC of $Fe_3O_4/IL/Ag$ and $Fe_3O_4/IL/Cu$ were 5-fold lower compared to $Fe_3O_4/IL/Au$. Similar results were observed for Staff with the same dosage. Optimized value of nanoparticles to MIC means that most of the cell were inactivated.

For investigation of catalyst morphology after test, SEM image was obtained. No change in morphology and structure was observed. This point indicate that the prepared catalysts are good candidates for bacteria cell walls destruction. Fig. 10. Demonstrate the SEM image of $Fe_3O_4/IL/Au$ after antibacterial test.

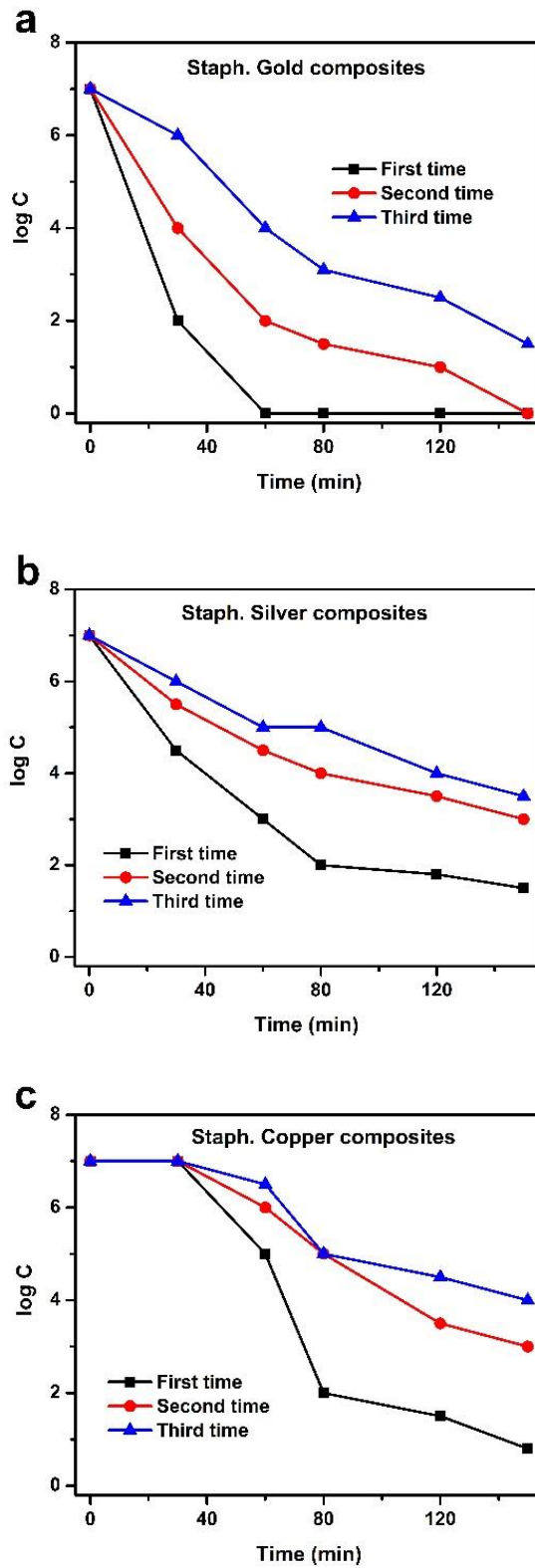


Fig. 8. Reuse ability of $\text{Fe}_3\text{O}_4/\text{IL}/\text{X}$. [catalyst]=750 ppm, [cell]= 10^7 CFU mL^{-1}

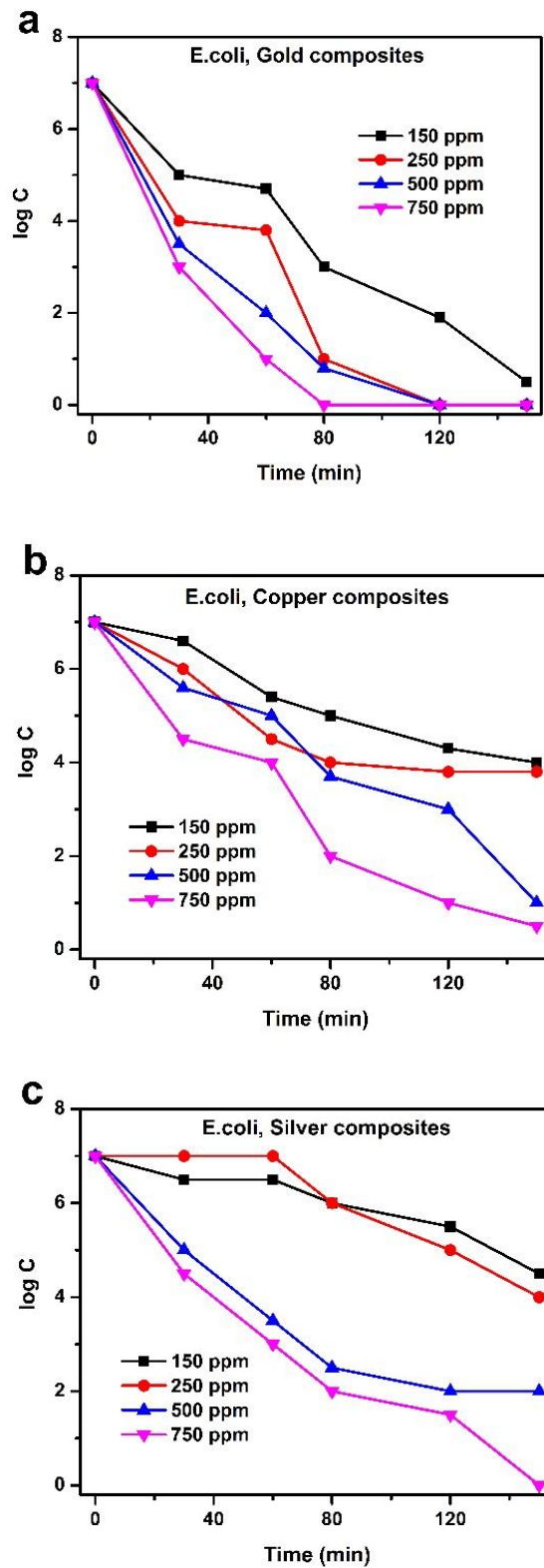


Fig. 9. MIC measurements of X/IL/Fe₃O₄. [cell]=10⁷ CFU mL⁻¹.

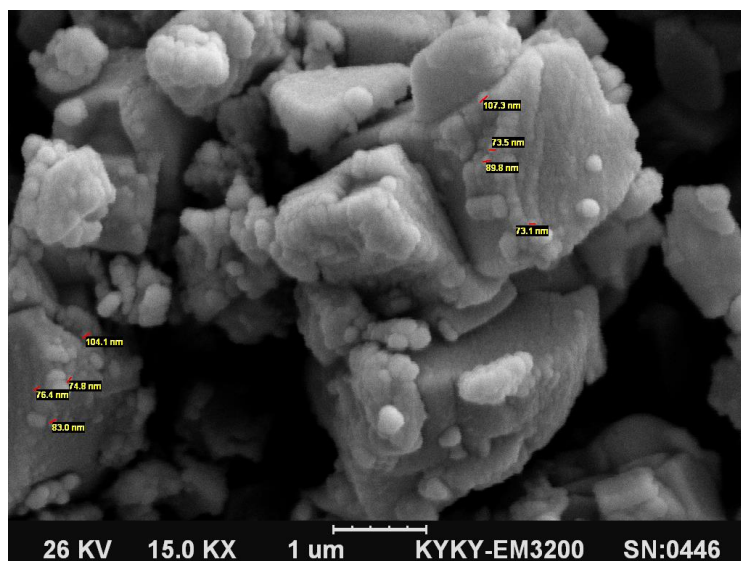


Fig. 10. SEM image of $\text{Fe}_3\text{O}_4/\text{IL}/\text{Au}$ after test.

CONCLUSION

In present research we evaluated the antibacterial activity of $\text{Fe}_3\text{O}_4/\text{IL}/\text{X}$ ($\text{X}=\text{Ag}, \text{Au}, \text{Cu}$) nanostructures. Cytotoxicity against *Escherichia coli* and *Staphylococcus aureus* was observed. Au, Cu and Ag adhere to the bacterial cell wall and penetrate through the cell membrane. Ionic liquid with forming hydrogen bond with cell wall create a channel that metals transferred to outer layer of bacteria. Both the MIC assay and TEM study demonstrated that $\text{Fe}_3\text{O}_4/\text{IL}/\text{Au}$ possessed higher microorganism inhibition compared to others.

CONFLICT OF INTEREST

The authors declare that there are no conflicts of interest regarding the publication of this manuscript.

REFERENCES

1. Padervand M, Vossoughi M. Fabrication and antibacterial performance of Ag–Au nanoparticles decorated ionic liquid modified magnetic core-shell microspheres. *Journal of Environmental Chemical Engineering*. 2014;2(4):1989-95.
2. Pankhurst QA, Connolly J, Jones SK, Dobson J. Applications of magnetic nanoparticles in biomedicine. *Journal of Physics D: Applied Physics*. 2003;36(13):R167-R81.
3. Gupta AK, Curtis ASG. Surface modified superparamagnetic nanoparticles for drug delivery: Interaction studies with human fibroblasts in culture. *Journal of Materials Science: Materials in Medicine*. 2004;15(4):493-6.
4. Neuberger T, Schöpf B, Hofmann H, Hofmann M, von Rechenberg B. Superparamagnetic nanoparticles for biomedical applications: Possibilities and limitations of a new drug delivery system. *Journal of Magnetism and Magnetic Materials*. 2005;293(1):483-96.
5. Perez JM, Simeone FJ, Saeiki Y, Josephson L, Weissleder R. Viral-Induced Self-Assembly of Magnetic Nanoparticles Allows the Detection of Viral Particles in Biological Media. *Journal of the American Chemical Society*. 2003;125(34):10192-3.
6. Graham DL, Ferreira HA, Freitas PP. Magnetoresistive-based biosensors and biochips. *Trends in Biotechnology*. 2004;22(9):455-62.
7. Padervand M, Vossoughi M, Yousefi H, Salari H, Gholami MR. An experimental and theoretical study on the structure and photoactivity of XFe_2O_4 ($\text{X} = \text{Mn}, \text{Fe}, \text{Ni}, \text{Co}, \text{and Zn}$) structures. *Russian Journal of Physical Chemistry A*. 2014;88(13):2451-61.
8. Monazam ER, Breault RW, Siriwardane R. Kinetics of Magnetite (Fe_3O_4) Oxidation to Hematite (Fe_2O_3) in Air for Chemical Looping Combustion. *Industrial & Engineering Chemistry Research*. 2014;53(34):13320-8.
9. Mehnert CP. Supported Ionic Liquid Catalysis. *Chemistry - A European Journal*. 2005;11(1):50-6.
10. Meidanshahi RV, Tasviri M, Khodadadi-Moghaddam M, Gholami MR. The synthesis of multiphase ionic liquid-coated $\text{Pt}/\text{Al}_2\text{O}_3$ catalysts: the selective synchronous hydrogenation of $\text{C}=\text{C}$ and $\text{C}=\text{O}$ bonds and the modeling of the ionic liquid and solvent effects. *Catal Sci Technol*. 2014;4(2):447-55.
11. Monsef R, Ghiyasiyan-Arani M, Salavati-Niasari M. Utilizing of neodymium vanadate nanoparticles as an efficient catalyst to boost the photocatalytic water purification. *Journal of Environmental Management*. 2019;230:266-81.
12. Monsef R, Ghiyasiyan-Arani M, Amiri O, Salavati-Niasari M. Sonochemical synthesis, characterization and application of PrVO_4 nanostructures as an effective photocatalyst for discoloration of organic dye contaminants in wastewater. *Ultrasonics Sonochemistry*. 2020;61:104822.
13. Ghiyasiyan-Arani M, Salavati-Niasari M. Strategic

- design and electrochemical behaviors of Li-ion battery cathode nanocomposite materials based on AlV3O9 with carbon nanostructures. *Composites Part B: Engineering*. 2020;183:107734.
14. Ghiyasiyan-Arani M, Salavati-Niasari M. New Nanocomposites Based on Li-Fe-Mn Double Spinel and Carbon Self-Doped Graphitic Carbon Nitrides with Synergistic Effect for Electrochemical Hydrogen Storage Application. *Industrial & Engineering Chemistry Research*. 2019;58(51):23057-67.
 15. Ghiyasiyan-Arani M, Salavati-Niasari M, Zonouz AF. Effect of Operational Synthesis Parameters on the Morphology and the Electrochemical Properties of 3D Hierarchical AlV3O9 Architectures for Li-Ion Batteries. *Journal of The Electrochemical Society*. 2020;167(2):020544.
 16. Abu-Reziq R, Wang D, Post M, Alper H. Platinum Nanoparticles Supported on Ionic Liquid-Modified Magnetic Nanoparticles: Selective Hydrogenation Catalysts. *Advanced Synthesis & Catalysis*. 2007;349(13):2145-50.
 17. Ivanova S, Bobadilla LF, Penkova A, Sarria FR, Centeno MA, Odriozola JA. Gold Functionalized Supported Ionic Liquids Catalyst for CO Oxidation. *Catalysts*. 2011;1(1):52-68.
 18. Sheldon R. ChemInform Abstract: Catalytic Reactions in Ionic Liquids. *ChemInform*. 2010;33(9):no-no.
 19. Salari H, Khodadadi-Moghaddam M, Harifi-Mood AR, Gholami MR. Preferential Solvation and Behavior of Solvatochromic Indicators in Mixtures of an Ionic Liquid with Some Molecular Solvents. *The Journal of Physical Chemistry B*. 2010;114(29):9586-93.
 20. Salari H, Harifi-Mood AR, Elahifard MR, Gholami MR. Solvatochromic Probes Absorbance Behavior in Mixtures of 2-Hydroxy Ethylammonium Formate with Methanol, Ethylene Glycol and Glycerol. *Journal of Solution Chemistry*. 2010;39(10):1509-19.
 21. Salari H, Hallett JP, Padervand M, Gholami MR. Systems Designed with an Ionic Liquid and Molecular Solvents to Investigate the Kinetics of an SNAr Reaction. *Progress in Reaction Kinetics and Mechanism*. 2013;38(2):157-70.
 22. Riisager A, Fehrmann R, Flicker S, van Hal R, Haumann M, Wasserscheid P. Very Stable and Highly Regioselective Supported Ionic-Liquid-Phase (SILP) Catalysis: Continuous-Flow Fixed-Bed Hydroformylation of Propene. *Angewandte Chemie International Edition*. 2005;44(5):815-9.
 23. Zhao X, Shi Y, Cai Y, Mou S. Cetyltrimethylammonium Bromide-Coated Magnetic Nanoparticles for the Preconcentration of Phenolic Compounds from Environmental Water Samples. *Environmental Science & Technology*. 2008;42(4):1201-6.
 24. Anderson JL, Armstrong DW. Immobilized Ionic Liquids as High-Selectivity/High-Temperature/High-Stability Gas Chromatography Stationary Phases. *Analytical Chemistry*. 2005;77(19):6453-62.
 25. Padervand M, Janatrostami S, Karanji AK, Gholami MR. Incredible antibacterial activity of noble metal functionalized magnetic core-zeolitic shell nanostructures. *Materials Science and Engineering: C*. 2014;35:115-21.
 26. Van Doorslaer C, Wahlen J, Mertens P, Binnemans K, De Vos D. Immobilization of molecular catalysts in supported ionic liquid phases. *Dalton Transactions*. 2010;39(36):8377.
 27. Padervand M, Reza Elahifard M, Vatan Meidanshahi R, Ghasemi S, Haghighi S, Reza Gholami M. Investigation of the antibacterial and photocatalytic properties of the zeolitic nanosized AgBr/TiO2 composites. *Materials Science in Semiconductor Processing*. 2012;15(1):73-9.
 28. Beveridge TJ. Ultrastructure, Chemistry, and Function of the Bacterial Wall. *International Review of Cytology: Elsevier*; 1981. p. 229-317.
 29. Beveridge TJ, Koval SF. Binding of metals to cell envelopes of *Escherichia coli* K-12. *Applied and Environmental Microbiology*. 1981;42(2):325-35.
 30. Feng QL, Wu J, Chen GQ, Cui FZ, Kim TN, Kim JO. A mechanistic study of the antibacterial effect of silver ions on *Escherichia coli* and *Staphylococcus aureus*. *Journal of Biomedical Materials Research*. 2000;52(4):662-8.
 31. Kim JY, Lee C, Cho M, Yoon J. Enhanced inactivation of *E. coli* and MS-2 phage by silver ions combined with UV-A and visible light irradiation. *Water Research*. 2008;42(1-2):356-62.
 32. Fox CL, Modak SM. Mechanism of Silver Sulfadiazine Action on Burn Wound Infections. *Antimicrobial Agents and Chemotherapy*. 1974;5(6):582-8.
 33. Arakawa H, Neault JF, Tajmir-Riahi HA. Silver(I) Complexes with DNA and RNA Studied by Fourier Transform Infrared Spectroscopy and Capillary Electrophoresis. *Biophysical Journal*. 2001;81(3):1580-7.
 34. Bragg PD, Rainnie DJ. The effect of silver ions on the respiratory chain of *Escherichia coli*. *Canadian Journal of Microbiology*. 1974;20(6):883-9.
 35. Neu HC, Chou J. Release of Surface Enzymes in Enterobacteriaceae by Osmotic Shock. *Journal of Bacteriology*. 1967;94(6):1934-45.
 36. Elahifard MR, Rahimnejad S, Haghighi S, Gholami MR. Apatite-Coated Ag/AgBr/TiO2 Visible-Light Photocatalyst for Destruction of Bacteria. *Journal of the American Chemical Society*. 2007;129(31):9552-3.
 37. Solioz M, Odermatt A. Copper and Silver Transport by CopB-ATPase in Membrane Vesicles of *Enterococcus hirae*. *Journal of Biological Chemistry*. 1995;270(16):9217-21.
 38. Klueh U, Wagner V, Kelly S, Johnson A, Bryers JD. Efficacy of silver-coated fabric to prevent bacterial colonization and subsequent device-based biofilm formation. *Journal of Biomedical Materials Research*. 2000;53(6):621-31.
 39. Raffi M, Mehrwan S, Bhatti TM, Akhter JI, Hameed A, Yawar W, et al. Investigations into the antibacterial behavior of copper nanoparticles against *Escherichia coli*. *Annals of Microbiology*. 2010;60(1):75-80.
 40. Cui Y, Zhao Y, Tian Y, Zhang W, Lü X, Jiang X. The molecular mechanism of action of bactericidal gold nanoparticles on *Escherichia coli*. *Biomaterials*. 2012;33(7):2327-33.